Application of the weak-field asymptotic theory to the analysis of tunneling ionization of linear molecules

Lars Bojer Madsen,[1] Oleg I. Tolstikhin,[2] and Toru Morishita[3]

[1]*Lundbeck Foundation Theoretical Center for Quantum System Research, Department of Physics and Astronomy, Aarhus University, Denmark*

[2]*National Research Center "Kurchatov Institute," Kurchatov Square 1, Moscow 123182, Russia*

[3]*Department of Engineering Science, The University of Electro-Communications, 1-5-1 Chofu-ga-oka, Chofu-shi, Tokyo 182-8585, Japan*

(Received 19 March 2012; published 3 May 2012)

The recently developed weak-field asymptotic theory [Phys. Rev. A **84**, 053423 (2011)] is applied to the analysis of tunneling ionization of a molecular ion (H_2^+), several homonuclear (H_2, N_2, O_2) and heteronuclear (CO, HF) diatomic molecules, and a linear triatomic molecule (CO_2) in a static electric field. The dependence of the ionization rate on the angle between the molecular axis and the field is determined by a structure factor for the highest occupied molecular orbital. This factor is calculated using a virtually exact discrete variable representation wave function for H_2^+, very accurate Hartree-Fock wave functions for the diatomics, and a Hartree-Fock quantum chemistry wave function for CO_2. The structure factors are expanded in terms of standard functions and the associated structure coefficients, allowing the determination of the ionization rate for any orientation of the molecule with respect to the field, are tabulated. Our results, which are exact in the weak-field limit for H_2^+ and, in addition, under the Hartree-Fock approximation for the diatomics, are compared with results from the recent literature.

DOI: 10.1103/PhysRevA.85.053404 PACS number(s): 32.80.Rm, 33.80.Rv, 42.50.Hz

I. INTRODUCTION

The orientation-resolved ionization yields from molecules have been addressed in an avalanche of recent experimental papers using intense femtosecond near-infrared laser pulses (see, e.g., Refs. [1–11]). The interest stems from the detailed information on strong-field dynamics contained in such alignment- or orientation-resolved data and the prospects for retrieving properties of the ionizing orbital, potentially even in a time-resolved way. So far, the experimental results have been compared against predictions of a molecular tunneling formula [molecular Ammosov-Delone-Krainov (MO-ADK)] [3,6–24], approximate numerical solution of the time-dependent Schrödinger equation (TDSE) [5,19,24–30], and the molecular strong-field approximation (MO-SFA) [13–15, 17,31–33]. In many cases the predictions differ even at the qualitative level, which is an unsatisfactory situation and a challenge for the theory.

The interest in tunneling ionization is also fed by the fact that it is the first step for rescattering and harmonic generation processes ignited by intense low-frequency laser pulses [34–36]. Recently it was realized [37,38] that photoelectron momentum distributions near the back-rescattering ridge and high-order harmonic generation spectra factorize into a product of the elastic scattering and photorecombination cross sections of the target, respectively, and a target-independent factor characterizing the flux of electrons arriving for rescattering. The conjecture of factorization, originally proposed in Ref. [37] on the basis of numerical solution of the TDSE, was confirmed by different theoretical methods for both photoelectron [39–41] and harmonic [42–44] spectra. It enables one to retrieve the target structure information, as was demonstrated experimentally for elastic scattering [45–48] and photorecombination [49–51] cross sections. The retrieving procedure again requires the knowledge of the orientation-resolved tunneling ionization rate of the target.

The problem of tunneling ionization in a static electric field is fundamental and has attracted attention since the early days of quantum mechanics [52]. While the general theory is formulated in terms of the solutions of the stationary Schrödinger equation satisfying the regularity and outgoing wave boundary conditions which can be constructed only numerically (see Ref. [53] and references therein), in the weak-field limit an asymptotic solution of the problem is possible. In this connection it is important to note a difference in terminology. In the case of a static field, the term "weak" is used if the interaction with the field can be treated perturbatively, while a time-dependent laser field with the same amplitude is usually referred to as "strong" in the tunneling regime of ionization. For atoms, the spherical symmetry simplifies the analysis and the weak-field asymptotic formulas for the ionization rate have been available for many years [54–58]. For hydrogen, even the next to the leading order in the field correction to the ionization rate for an arbitrary state was obtained [59]. For molecules, the multicenter nature of the ionizing orbital complicates the analysis. A breakthrough came with the so-called MO-ADK formula [12], which was constructed by *analogy* with the atomic case [56,60] rather than derived from the Schrödinger equation. In contrast to the atomic case, the region of validity of this formula for the lack of its derivation remained unclear. For the same reason such an important physical factor as the linear Stark shift caused by a permanent dipole moment of the ionizing orbital was missed.

In our recent work [61], the asymptotic theory of tunneling ionization in a weak electric field was reconsidered. A consistent approach to the problem based on the adiabatic expansion in parabolic coordinates [53] was developed. The previously known asymptotic formulas for the atomic case [54–58] were rederived and the correct leading-order asymptotics for the ionization rate of molecules was obtained. In contrast to the original MO-ADK formula [12], our theory accounts for the possible existence of a permanent dipole moment of the

ionizing orbital and hence is invariant under translations of the coordinate origin. It classifies the different contributions to the ionization rate by the power of the field in the pre-exponential factor, thus attributing them to the different orders of the asymptotic expansion, and introduces the notion of a dominant channel which is the only one to be retained in the leading-order approximation. The ionization rate in this approximation is shown to factorize into a product of what is called the *structure factor*, which depends only on the orientation of the molecule with respect to the field, and a simple analytically known function of the field. While the previous paper [61] was devoted to developing and validating the theory, in the present work we discuss its applications. Our goal here is to illustrate the implementation of the theory and provide a set of reliable results for tunneling ionization in the weak-field limit. Since the dependence on the field in this limit is trivial, we focus on the orientation-dependent structure factor. It is determined by the behavior of the unperturbed wave function of the tunneling electron in the asymptotic region. We present results for a number of small linear polar and nonpolar molecules of current theoretical and experimental interest obtained from wave functions at different levels of approximation and compare them with the recent literature.

The paper is organized as follows. In Sec. II, we list the formulas needed to evaluate the tunneling ionization rate within the weak-field asymptotic theory [61]. In Sec. III, we present and discuss our results. We begin with the benchmark results for H_2^+ obtained from a virtually exact wave function constructed using a discrete variable representation [62] in prolate spheroidal coordinates [63]. Then we consider diatomic molecules H_2, N_2, CO, O_2, and HF with different symmetry of the highest occupied molecular orbital (HOMO). The HOMOs for these molecules are obtained using a very accurate program X2DHF [64,65] implementing the Hartree-Fock method for diatomic molecules and correctly accounting for the asymptotic form of the wave function. Finally we illustrate the performance of less accurate in the asymptotic region quantum chemistry wave functions by the results for a linear triatomic molecule CO_2 using the code GAMESS [66]. The conclusions and an outlook are formulated in Sec. IV.

II. THEORY

In this section, we recapitulate the formulas needed to apply the weak-field asymptotic theory of tunneling ionization of molecules [61]. In this theory, a molecule is treated in the single-active-electron approximation. For all molecules considered in the present paper, the active electron will be described by the HOMO. To find the ionization rate, one needs the field-free energy E_0, wave function $\psi_0(\mathbf{r})$, and dipole moment $\boldsymbol{\mu}$ of the active electron given by (atomic units are used throughout)

$$\boldsymbol{\mu} = -\int \psi_0^*(\mathbf{r})\mathbf{r}\psi_0(\mathbf{r})\,d\mathbf{r}. \tag{1}$$

We use the notation

$$\varkappa = \sqrt{2|E_0|}. \tag{2}$$

The direction of the external electric field $\mathbf{F}$ defines the laboratory frame. We choose a geometry where the field is always pointing in the positive z direction of the laboratory frame, so $\mathbf{F} = F\mathbf{e}_z$, $F > 0$. The orientation of the molecule is specified by the three Euler angles (α,β,γ) defining a rotation from the laboratory frame to a molecular frame, where α is the angle of rotation around the laboratory z axis, β is the angle of rotation around the new y axis, and γ is the angle of rotation around the molecular z axis [67]. The wave function and dipole moment are assumed to be originally given in the molecular frame; then $\psi_0(\mathbf{r})$ and $\boldsymbol{\mu}$ are obtained by applying the rotation. Thus, the dependence on (α,β,γ) is implicitly contained in $\psi_0(\mathbf{r})$ and $\boldsymbol{\mu}$. Since the field is axially symmetric in the laboratory frame, the ionization rate does not depend on α, so we set $\alpha = 0$. Since the field is homogeneous, the ionization rate does not depend on the position of the origin of the coordinate system used to define $\psi_0(\mathbf{r})$ and $\boldsymbol{\mu}$. The latter invariance is an important issue in the theory [61] and is used below.

A. Weak-field asymptotics

The theory of tunneling ionization of molecules can be formulated as a multichannel eigenvalue problem in parabolic coordinates (ξ,η,φ) [53,61]. In the weak-field limit, the total ionization rate is given by [61]

$$\Gamma = \sum_{n_\xi=0}^{\infty}\sum_{m=-\infty}^{\infty}\Gamma_{n_\xi m} + O(\Gamma^2), \tag{3}$$

where $\Gamma_{n_\xi m}$ is the partial rate for ionization into a channel with parabolic quantum numbers n_ξ and m. The asymptotics of $\Gamma_{n_\xi m}$ for $F \to 0$ has the form [61]

$$\Gamma_{n_\xi m} = |G_{n_\xi m}(\beta,\gamma)|^2 W_{n_\xi m}(F)[1 + O(F)], \tag{4}$$

where the leading-order term is defined by

$$G_{n_\xi m}(\beta,\gamma) = e^{-\varkappa\mu_z} g_{n_\xi m}(\beta,\gamma) \tag{5}$$

and

$$W_{n_\xi m}(F) = \frac{\varkappa}{2}\left(\frac{4\varkappa^2}{F}\right)^{2Z/\varkappa-2n_\xi-|m|-1}\exp\left(-\frac{2\varkappa^3}{3F}\right). \tag{6}$$

Here Z is the charge in the Coulomb tail of the one-electron potential supporting the orbital $\psi_0(\mathbf{r})$, $\mu_z = \mathbf{e}_z\boldsymbol{\mu}$ is the z component of $\boldsymbol{\mu}$, and $g_{n_\xi m}(\beta,\gamma)$ is the asymptotic coefficient in the expansion of $\psi_0(\mathbf{r})$ in terms of the parabolic basis defined by the projection

$$g_{n_\xi m}(\beta,\gamma) = \sqrt{\frac{\varkappa^{|m|+1}}{|m|!}}\,\eta^{1+|m|/2-Z/\varkappa}e^{\varkappa\eta/2} \times \int_0^\infty\int_0^{2\pi}\phi_{n_\xi|m|}(\xi)\frac{e^{-im\varphi}}{\sqrt{2\pi}}\psi_0(\mathbf{r})\,d\xi\,d\varphi\Big|_{\eta\to\infty} \tag{7}$$

The channel functions $\phi_{n_\xi|m|}(\xi)$ are explicitly given by

$$\phi_{n_\xi|m|}(\xi) = \varkappa^{1/2}(\varkappa\xi)^{|m|/2}e^{-\varkappa\xi/2}\sqrt{\frac{n_\xi!}{(n_\xi+|m|)!}}\,L_{n_\xi}^{(|m|)}(\varkappa\xi), \tag{8}$$

where $L_n^{(\alpha)}(x)$ are the generalized Laguerre polynomials [68]. They satisfy

$$\int_0^\infty \phi_{n_\xi|m|}(\xi)\phi_{n'_\xi|m|}(\xi)\,d\xi = \delta_{n_\xi n'_\xi}. \tag{9}$$

An important consequence of Eq. (4) is that in the leading-order approximation the partial rate $\Gamma_{n_\xi m}$ factorizes into two factors, one of which depends only on the orientation angles (β,γ) and the other depends only on the field F. We recall that the dependence of the right-hand sides of Eqs. (5) and (7) on (β,γ) is contained in μ_z and $\psi_0(\mathbf{r})$. The orientation-dependent structure factor $G_{n_\xi m}(\beta,\gamma)$ is the most important characteristic which should be extracted from the active electron's orbital. It is given by a product of an exponential factor depending on μ_z and the asymptotic coefficient $g_{n_\xi m}(\beta,\gamma)$ characterizing $\psi_0(\mathbf{r})$. Only this product is invariant under translations of the coordinate origin; each of the factors is not [61]. We mention that the standard MO-ADK formula [12] does not account for a permanent dipole moment of the active electron, and hence its predictions for molecules with nonzero $\boldsymbol{\mu}$ depend on the choice of the origin. The field-dependent factor $W_{n_\xi m}(F)$ is a simple function which depends on the molecule only via Z and $\varkappa$.

The bound-state wave function $\psi_0(\mathbf{r})$ can always be chosen to be real. Then

$$G_{n_\xi,-|m|}(\beta,\gamma) = G^*_{n_\xi,|m|}(\beta,\gamma), \quad \Gamma_{n_\xi,-|m|} = \Gamma_{n_\xi,|m|}, \tag{10}$$

and Eq. (3) takes the form

$$\Gamma = \sum_{n_\xi=0}^{\infty}\left[\Gamma_{n_\xi 0} + 2\sum_{m=1}^{\infty}\Gamma_{n_\xi m}\right] + O(\Gamma^2). \tag{11}$$

In the following, we assume that this is the case and consider only channels with $m \geqslant 0$. The channels are referred to by (n_ξ,m).

B. Dominant channels

The equations given in the previous section are sufficient. However, we feel that it is worthwhile to clarify some aspects of the asymptotic theory [61] which may raise questions in applications. It is important to realize the fact that the ionization rate Γ is obtained as an asymptotic expansion for $F \to 0$ and understand the structure of this expansion. First, as can be seen from Eq. (6), for $F \to 0$ the error term $O(\Gamma^2)$ in Eq. (3) is exponentially smaller than not only the total rate Γ, but also each of the partial rates $\Gamma_{n_\xi m}$. This term therefore should be neglected independently of how many partial rates are retained in the sum. Second, the different partial rates have different powers of F in Eq. (6), and the dominant for $F \to 0$ channel corresponds to the minimum values of n_ξ and m present in the sum. Third, Eqs. (5) and (6) define only the leading-order term in the asymptotics of $\Gamma_{n_\xi m}$. So it is inconsistent to include higher channels unless corrections of the same order are taken into account in Eq. (4) for the dominant channel. All this means that in the leading-order approximation only the dominant channel is to be retained in Eq. (11).

Although the main focus in this work is on linear molecules, we include a discussion of the general case of nonlinear molecules for completeness. For nonlinear molecules, the dominant channel generally is (0,0), and we have from Eqs. (4) and (11)

$$\Gamma \approx |G_{00}(\beta,\gamma)|^2 W_{00}(F). \tag{12}$$

There may exist specific orientations (β_0,γ_0) related to nodal lines and nodal surfaces of the wave function $\psi_0(\mathbf{r})$, where $g_{00}(\beta_0,\gamma_0) = 0$ and $g_{01}(\beta_0,\gamma_0) \neq 0$. For such an orientation the dominant channel is (0,1), and we have

$$\Gamma \approx 2|G_{01}(\beta_0,\gamma_0)|^2 W_{01}(F). \tag{13}$$

The situation when the orientation (β,γ) of the molecule is close to (β_0,γ_0) is the only case when the two channels in Eq. (11) can be summed up without introducing an inconsistency. Thus, for orientations near (β_0,γ_0) we have

$$\begin{aligned}\Gamma &\approx |G_{00}(\beta,\gamma)|^2 W_{00}(F) + 2|G_{01}(\beta,\gamma)|^2 W_{01}(F)\\ &\approx \left[|G_{00}(\beta,\gamma)|^2 + \frac{F}{2\varkappa^2}\,|G_{01}(\beta,\gamma)|^2\right] W_{00}(F).\end{aligned} \tag{14}$$

This formula remains consistent as (β,γ) departs from (β_0,γ_0) up to the moment when the two terms become comparable, and the size of the region where the channel (0,1) should be retained decreases as $F \to 0$. We note that channels with $n_\xi \neq 0$ never can be dominant, since the integral in Eq. (7) for a given m and $n_\xi = 0$ is generally nonzero.

Let us mention an issue related to the notion of the dominant channel. In this work, we do not consider contributions to the ionization rate from the next-highest occupied molecular orbital, the HOMO-1. As is clear from the above discussion, the role of the HOMO-1 in the ionization dynamics requires special attention near the orientations where the contribution to ionization from the dominant channel of HOMO vanishes [15].

Linear molecules require a special consideration. In this case, the unperturbed bound-state wave function $\psi_0(\mathbf{r})$ is characterized by the projection of the electronic angular momentum onto the molecular axis which is denoted by M. The energy of the state does not depend on the sign of M, so the states with $M \neq 0$ are degenerate. This degeneracy is removed by an arbitrarily weak field, provided that the molecular axis does not coincide with the direction of the field. The correct bound-state wave functions of the zeroth order are certain linear combinations of the two degenerate states [54]. If the molecular axis is rotated by an angle β in the xz plane of the laboratory frame, one of these states is even with respect to the plane of rotation and the other is odd. The states with $M = 0$ (σ states) belong to the class of even states. For both even and odd states, the factors $G_{n_\xi m}(\beta,\gamma)$ in Eq. (4) do not depend on γ; therefore, for linear molecules we use the simplified notation $G_{n_\xi m}(\beta)$. For even states, the dominant channel is (0,0), and we have

$$\Gamma \approx |G_{00}(\beta)|^2 W_{00}(F). \tag{15}$$

For odd states $g_{00}(\beta) = 0$; hence, the dominant channel is (0,1), and we have

$$\Gamma \approx 2|G_{01}(\beta)|^2 W_{01}(F). \tag{16}$$

Near an orientation β_0, where $g_{00}(\beta_0) = 0$ and $g_{01}(\beta_0) \neq 0$ (for example, $\beta_0 = 0$ and π for even states with $M \neq 0$), the two terms can be summed up similarly to Eq. (14),

$$\Gamma \approx \left[|G_{00}(\beta)|^2 + \frac{F}{2\varkappa^2}\,|G_{01}(\beta)|^2\right] W_{00}(F). \tag{17}$$

In the particular case of states with $|M| = 1$ (π states), the wave function $\psi_0(\mathbf{r})$ has a nodal plane. For $\beta = 0$, the nodal

plane of the even state coincides with the yz plane, and the nodal plane of the odd state coincides with the xz plane. In this case it is convenient to identify the states by the nodal plane and denote the even and odd states by (yz) and (xz), respectively. We use this notation in Sec. III in the discussion of the results.

C. Expansion of the structure factors

Let us reiterate that the dependence of the ionization rate on the orientation (β,γ) of the molecule with respect to the field is determined by the structure factors (5). In the present leading-order approximation, a single factor corresponding to the dominant channel is needed to implement the theory. However, its values are needed for all possible orientations of the molecule. This factor as a function of the orientation can be expanded in terms of an appropriate set of standard functions. This may help to compress the information needed for applications and facilitate its exchange between researches.

In the general case of nonlinear molecules, the structure factors $G_{n_\xi m}(\beta,\gamma)$ can be expanded as

$$G_{n_\xi m}(\beta,\gamma) = \sum_{lm'} C^{(lm')}_{n_\xi m} Y_{lm'}(\beta,\gamma), \tag{18}$$

where

$$Y_{lm}(\beta,\gamma) = \Theta_{lm}(\beta)\,\frac{e^{im\gamma}}{\sqrt{2\pi}} \tag{19}$$

are spherical harmonics and $\Theta_{lm}(\beta)$ is given in terms of the associated Legendre polynomials $P^m_l(x)$ by

$$\Theta_{lm}(\beta) = \sqrt{\frac{(2l+1)(l-m)!}{2(l+m)!}}\,P^m_l(\cos\beta). \tag{20}$$

We use the Condon-Shortley [69] phase convention for $\Theta_{lm}(\beta)$, that is,

$$\Theta_{l-m}(\beta) = (-1)^m \Theta_{lm}(\beta). \tag{21}$$

The structure factor for the dominant channel $G_{00}(\beta,\gamma)$ is real, so we have

$$C^{(l-m')}_{00} = (-1)^{m'} C^{(lm')*}_{00}. \tag{22}$$

For linear molecules there is no dependence on γ, and the structure factors $G_{n_\xi m}(\beta)$ can be expanded in the form

$$G_{n_\xi m}(\beta) = i^p \sum_{l=|M-m|}^{\infty} C^{(l)}_{n_\xi m}\Theta_{l|M-m|}(\beta). \tag{23}$$

For even states $M \geqslant 0$, $m \geqslant 0$, and $p = 0$; for odd states $M \geqslant 1$, $m \geqslant 1$ [from $g_{n_\xi 0}(\beta) = 0$ we have $C^{(l)}_{n_\xi 0} = 0$], and $p = 1$. The *structure coefficients* $C^{(lm')}_{n_\xi m}$ and $C^{(l)}_{n_\xi m}$ in the expansions (18) and (23) can be tabulated for the molecules under investigation and then used for calculating the structure factors (5). Given these coefficients, the application of the present theory becomes straightforward. This approach is especially efficient if expansions (18) and (23) rapidly converge, which is the case for all molecules considered below.

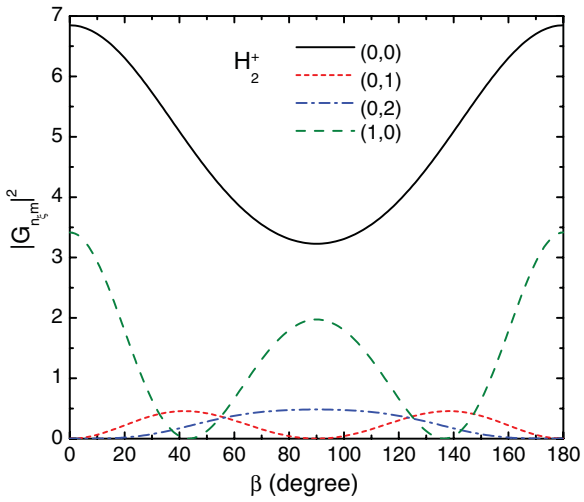

FIG. 1. (Color online) The dependence of the structure factors on the angle β between the internuclear axis and the electric field [see Eqs. (4) and (5)] for the ground $1s\sigma_g$ state of H_2^+ with nuclei fixed at a distance $R = 2$. The different channels are indicated by (n_ξ,m). The dominant channel (0,0) is shown by solid black curve.

III. RESULTS AND DISCUSSION

In this section we present the results for structure factors $G_{n_\xi m}(\beta)$ as functions of the angle β between the molecular axis and the field for a number of linear molecules. As follows from Eq. (7), to implement the weak-field asymptotic theory [61] we need an approach capable of accurately describing the asymptotic behavior of $\psi_0(\mathbf{r})$ at large η. We begin with the simplest one-electron molecular system H_2^+ for which a virtually exact wave function can be obtained. Then we consider several many-electron diatomic molecules H_2, N_2, CO, O_2, and HF in the Hartree-Fock approximation. Following Ref. [14], the HOMOs in these molecules are constructed by solving the Hartree-Fock equations using X2DHF [64,65]. To extend applications of the theory to polyatomic molecules, it is natural to try to use standard quantum chemistry codes based on an expansion of the active orbital in terms of Gaussian basis functions placed at the different atomic centers. Because of the difficulty in reproducing the exponentially decaying tail of the wave function by the Gaussian basis, such codes cannot be expected to be very suitable for the present purposes. We illustrate what can be achieved in this approach by the example of CO_2 with the HOMO obtained from GAMESS [66].

A. Hydrogen molecular ion: Benchmark results

The hydrogen molecular ion is an excellent test ground for illustrating the theory [61]. For this molecule $Z = 2$ and $\boldsymbol{\mu} = \mathbf{0}$ in the center-of-mass frame. We have performed a very accurate calculation of the ground $1s\sigma_g$ state of H_2^+ for a fixed internuclear distance $R = 2$ using discrete variable representations (DVRs) based on Jacobi and Laguerre polynomials [62] for prolate spheroidal coordinates η and ξ [63], respectively. The bound-state energy $E_0 = -1.102\,634\,214\,5$ obtained by this method agrees in all significant digits with that from X2DHF [64,65].

Figure 1 shows the results for H_2^+ obtained using the DVR wave function. The wave function from X2DHF [64,65] gives

TABLE I. Structure coefficients for the dominant channel (0,0) for the ground $1s\sigma_g$ state of H_2^+ with $R = 2$ using the DVR wave function. $a[b] = a \times 10^b$.

l	$C_{00}^{(l)}$
0	2.910
2	0.340
4	0.980[−2]
6	0.130[−3]
8	0.221[−5]

results which look identical. The present procedure to extract the structure factors $G_{n_\xi m}(\beta)$ from the wave function $\psi_0(\mathbf{r})$ is described in the next section. In the figure, we plot the absolute values squared of $G_{n_\xi m}(\beta)$ for several lowest channels with $(n_\xi, m) = (0,0)$, $(0,1)$, $(0,2)$, and $(1,0)$. The orientation dependence of the ionization rate in the weak-field limit is determined by the contribution from the dominant channel (0,0) [see Eq. (15)]. The structure coefficients $C_{00}^{(l)}$ in Eq. (23) for this channel are given in Table I. From the figure, we see that $|G_{00}(\beta)|^2$ peaks at $\beta = 0^\circ$ and 180°, when the field is parallel to the molecular axis, and has a minimum at $\beta = 90^\circ$. This behavior reflects the fact that the charge density is elongated along the internuclear axis, which is common for σ states in other homonuclear molecules discussed below. This behavior was also found in TDSE calculations performed in the tunneling regime [70,71]. The structure factors for higher channels are shown to illustrate that the different partial rates have different orientation dependencies. Their contributions to the total ionization rate cannot be simply added to that from the dominant channel, as explained in Sec. II B. One can see from Eq. (6) that in the weak-field limit the contribution from channel $(0,1)$ is smaller by a factor of F and that the contributions from channels (0,2) and (1,0) are smaller by a factor of F^2. If a correction of order $O(F)$ in Eq. (4) for the dominant channel (0,0) were obtained, one could include the contribution from channel $(0,1)$ having the same order. As far as we know, such a correction is available only for the hydrogen atom [59]. The present results for the dominant channel are very accurate and may serve as a benchmark for testing future calculations of the tunneling ionization rate of H_2^+ in a weak static electric field.

B. Diatomic molecules: Hartree-Fock wave functions with correct asymptotic behavior

The agreement between the X2DHF and the DVR results for H_2^+ supports the accuracy of both methods. For many-electron diatomic molecules we performed additional Hartree-Fock calculations using GAMESS [66] to compare the energies and dipole moments. For each molecule the nuclei were placed at the experimental equilibrium distance given by the NIST Computational Chemistry Comparison and Benchmark Database [72]. Table II gives the energies of the HOMO obtained with the two methods. The agreement between the energies is generally very good except for the triplet ground state in O_2. In this case, the difference in the HOMO energy is attributed to the difference between the restricted open-shell Hartree-Fock (ROHF) method [64,65] in X2DHF and the unrestricted Hartree-Fock (UHF) method in GAMESS [66]. However, the total electron energy of the O_2 molecule agrees well in the two methods, −149.6675 with the ROHF method and −149.6781 with the UHF method, illustrating that only the total energy is well-defined for open-shell molecules.

TABLE II. HOMO energies (in atomic units) for selected molecules. The GAMESS calculations were performed with the augmented correlation-consistent valence triple ζ (aug-cc-TZV) basis set.

Method	N_2	O_2	CO	HF
X2DHF [64,65]	−0.6345	−0.5324	−0.5549	−0.6504
GAMESS [66]	−0.6346	−0.5594	−0.5549	−0.6506

The wave function and dipole from X2DHF are originally given in the geometrical-center frame. For homonuclear molecules, the geometrical-center and center-of-mass frames coincide, but for heteronuclear molecules they do not. Our theory is invariant under translation of the origin, so any frame can be used in the calculations. We have checked that the results for heteronuclear molecules do not depend on the choice of frame. Table III gives the dipoles of the HOMO of CO and HF with respect to the center of mass, and the agreement between the two methods is fairly good.

1. *Molecules with HOMOs of σ symmetry*

We first focus on molecules with HOMOs of σ symmetry and consider H_2, N_2, and CO. In Figs. 2–4 we show the orientation dependence of the structure factors $|G_{n_\xi m}(\beta)|^2$ for the (0,0) and (0,1) channels for each molecule. Table IV gives the structure coefficients $C_{00}^{(l)}$.

Figure 2 shows $|G_{00}(\beta)|^2$ and $|G_{01}(\beta)|^2$ for H_2. The small variation in $|G_{00}(\beta)|^2$ with the angle β reflects that the shape of the HOMO is nearly spherically symmetric. There has recently been quite some interest in the orientation dependence of the ionization yield for H_2. The ratio between the ionization yields at $\beta = 0^\circ$ and $\beta = 90^\circ$ was measured in two different strong-field ionization experiments using a wavelength of 800 nm [17] and 1850 nm [27], respectively. In Ref. [17] a value of 1.32 was obtained for this ratio at an intensity of 2.3×10^{14} W/cm^2 and a smaller value of 1.17 at a higher intensity of 4.5×10^{14} W/cm^2. In Ref. [27] a ratio of 1.15 was measured at 2×10^{14} W/cm^2. Recent TDSE calculations within the single-active-electron model reported ratios decreasing from 1.3 to 1.1 with increasing intensity [24], which is a predicted trend in qualitative agreement with the experimental results. The value for this ratio predicted by the standard MO-ADK formula [12]

TABLE III. HOMO dipole moments (in atomic units) for selected molecules in the center-of-mass molecular frame. $\hat{z}$ is a unit vector in the direction of the molecular z axis. For CO and HF, O and F are on the positive side of this axis, respectively. The GAMESS calculations were performed with the aug-cc-TZV basis set.

Method	CO	HF
X2DHF [64,65]	1.72 $\hat{z}$	−0.0383 $\hat{z}$
GAMESS [66]	1.72 $\hat{z}$	−0.0386 $\hat{z}$

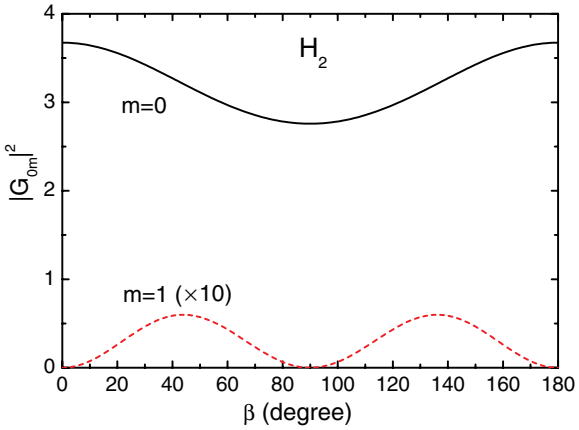

FIG. 2. (Color online) The dependence of the structure factors on the angle β between the internuclear axis and the electric field [see Eqs. (4) and (5)] for the ground state in H_2 of σ_g symmetry. Solid (black) curve, $m = 0$; dashed (red) curve, $m = 1$. The nuclei are fixed at the experimental equilibrium distance.

was given to be 1.17 in Refs. [17,27]. A later work revised the MO-ADK calculation and adjusted the value to around 1.4 [19]. Our value for the ratio, 1.33, is accurate in the weak-field limit and should be used as a reference rather than the multitude of different MO-ADK values.

We now turn to the results for N_2. We first note that the energy of the $1\pi_u$ orbital is slightly higher than the $3\sigma_g$ orbital in the Hartree-Fock approximation. However, experimental photoelectron spectra [73] show that single ionization leaves the cation in a Σ_g state, and hence the correct orbital to choose for the HOMO is the $3\sigma_g$. As seen in Fig. 3 also for N_2, the structure factor $|G_{00}(\beta)|^2$ peaks at $\beta = 0^\circ$ and $\beta = 180^\circ$ and has a minimum at 90°. Compared to H_2 the variation in the orientation dependence of $|G_{00}(\beta)|^2$ is larger. This difference can be explained by noting that the HOMO of N_2 has a shape that is more elongated along the molecular axis than is the case with the HOMO of H_2. The prediction of maxima in the structure factor at $\beta = 0^\circ$ and $\beta = 180^\circ$ and a minimum at $\beta = 90^\circ$ agrees with the results found in measurements

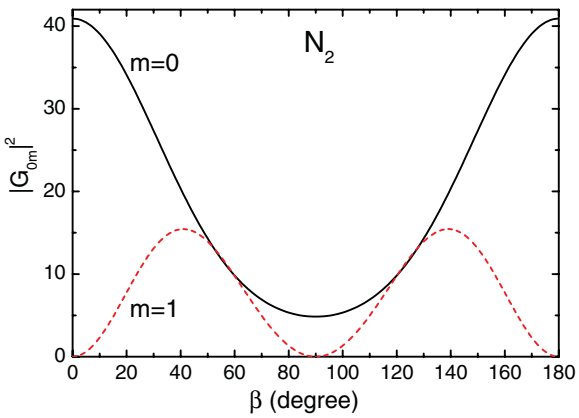

FIG. 3. (Color online) The dependence of the structure factors on the angle β between the internuclear axis and the electric field [see Eqs. (4) and (5)] for the HOMO in N_2 of σ_g symmetry. Solid (black) curve, $m = 0$; dashed (red) curve, $m = 1$. The nuclei are fixed at the experimental equilibrium distance.

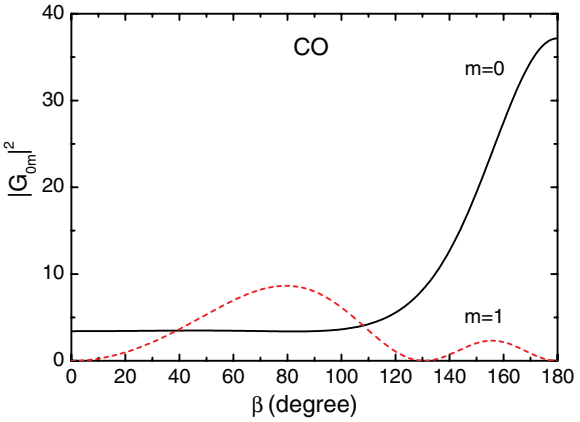

FIG. 4. (Color online) The dependence of the structure factors on the angle β between the internuclear axis and the electric field [see Eqs. (4) and (5)] for the HOMO in CO of σ symmetry. The C (O) atom is on the negative (positive) z axis in the molecular fixed frame. Solid (black) curve, $m = 0$; dashed (red) curve, $m = 1$ channel. The nuclei are fixed at the experimental equilibrium distance.

performed with intense femtosecond near-infrared laser pulses [1–3], as well as with predictions from the MO-ADK [3,13,20], the MO-SFA [13,32], time-dependent density-functional calculations [74], and an approach based on the TDSE with contributions from multiple orbitals [30]. We find the ratio between the $|G_{00}(\beta)|^2$ at $\beta = 0^\circ$ and $\beta = 90^\circ$ to be 8.44, which is somewhat larger than the experimental value of 4 reported in Ref. [1], but close to the value found in previous calculations [13].

As a last example of a diatomic molecule with a HOMO of σ symmetry we consider CO, which has a permanent dipole. Recent combined experimental and theoretical studies showed the importance of the permanent dipole in strong-field ionization [6–8,10,11,75], and it is therefore interesting to consider the predictions of the weak-field asymptotic theory for polar molecules. In CO the HOMO has an excess charge on the C atom, so that the dipole in Eq. (1) with respect to the center of mass is nonvanishing and points from C to O. In Table III the dipole associated with the HOMO is given in the center-of-mass frame. In Fig. 4 we see that $|G_{00}(\beta)|^2$ is almost constant from $\beta = 0^\circ$ and up to $\beta = 90^\circ$. It then monotonically

TABLE IV. Structure coefficients $C_{00}^{(l)}$ for diatomic molecules in σ states ($M = 0$) using a X2DHF wave function [64,65]. $a[b] = a \times 10^b$.

l	H_2	N_2	CO
0	2.468	4.972	3.330
1			−0.974
2	0.107	1.729	0.791
3			−0.439
4	0.104[−2]	0.678[−1]	0.160
5			−0.449[−1]
6	0.465[−5]	0.930[−3]	0.104[−1]
7			−0.206[−2]
8		0.149[−4]	0.357[−3]
9			−0.551[−4]
10			0.777[−5]

TABLE V. Structure coefficients $C_{00}^{(l)}$ for diatomic molecules in even π states ($M = 1$) using a X2DHF wave function [64,65]. $a[b] = a \times 10^b$.

l	$O_2(yz)$	HF(yz)
1		2.227
2	1.438	0.227
3		0.519[–1]
4	0.604[–1]	0.968[–2]
5		0.156[–2]
6	0.785[–3]	0.219[–3]
7		0.269[–4]
8	0.541[–5]	0.293[–5]

TABLE VI. Structure coefficients $C_{01}^{(l)}$ for diatomic molecules in odd π states ($M = 1$) using a X2DHF wave function [64,65]. $a[b] = a \times 10^b$.

l	$O_2(xz)$	HF(xz)
0		2.592
1	2.311	0.347
2		0.852[–1]
3	0.107	0.164[–1]
4		0.270[–2]
5	0.145[–2]	0.383[–3]
6		0.475[–4]
7	0.104[–4]	0.527[–5]

increases and peaks at $\beta = 180^\circ$, where the dipole of the HOMO is antiparallel to the field. In the conventional MO-ADK model [12], the orientation dependence of the rate is just the opposite to the one shown in Fig. 4 [10,16,21]. This wrong prediction can be understood in terms of the excess charge on the C atom compared to the O atom with lack of permanent dipole effect: When the field points from C to O there is simply more charge close to the tunnel exit, and ionization is expected to occur more readily. When the permanent dipole is included in the MO-ADK by accounting for the associated Stark shift, that formalism predicts a result in qualitative agreement with the present findings [10]. We note that there are several discussions of the strong-field ionization of polar molecules in terms of the total permanent dipole of the molecule, the dipole of the probed orbital, and the dipole from the single-active-electron potential [29]. The orientation dependence of the ionization yield for the CO molecule was recently addressed experimentally using linearly polarized two-color near-infrared intense femtosecond laser pulses [9,10]. The measurements showed a dominant ionization at $\beta = 0^\circ$, where $|G_{00}(\beta)|^2$ is smallest. We note that the low-energy electrons produced by a linearly polarized laser pulse are strongly affected by postionization dynamics [29]. To exclude effects of field-induced rescattering of the tunneled electron with the core, strong-field ionization from oriented polar molecules in circularly polarized light is an attractive experimental approach [6–8,11]. Also for atoms the use of circularly polarized light can be advantageous. For example, the effect on the photoelectron momentum distribution of the dipole potential induced by the polarization of the inner core electrons was recently identified using close to circularly polarized light [76,77]. Further studies would be needed to understand the ionization dynamics of polar molecules under experimental conditions.

2. *Molecules with HOMOs of π symmetry*

For molecules with HOMOs of π symmetry there are two degenerate states, even (yz) and odd (xz), as defined in Sec. II A. Here, (yz) and (xz) denote the nodal planes of the orbitals at $\beta = 0^\circ$. In the figures below we show the structure factors $|G_{0m}(\beta)|^2$ ($m = 0,1,2$) for both even and odd states for O_2 and HF. In Tables V and VI the structure coefficients $C_{0m}^{(l)}$ are given for $m = 0$ and $m = 1$, respectively.

In Fig. 5, we show the orientation dependence of $|G_{0m}(\beta)|^2$ for the π_g HOMO of O_2. The top panel shows results for the (0,0) and (0,1) channels for the even (yz) HOMO. The bottom panel shows the results for the odd (xz) HOMO in the (0,1) and (0,2) channels. From the figure, we see that the dominant channel (0,0) has minima at 0°, 90°, and 180° and maxima at ≃42° and 138°. This prediction is in qualitative agreement with previous MO-ADK [3,12,16,20,21], TDSE [30], and time-dependent density-functional calculations [78], as well as with the findings from strong-field ionization experiments [3]. The qualitative shape of the orientational dependence in the (0,0) channel as seen in Fig. 5 with two peaks between the minima at 0°, 90°, and 180° is generic for linear molecules with a

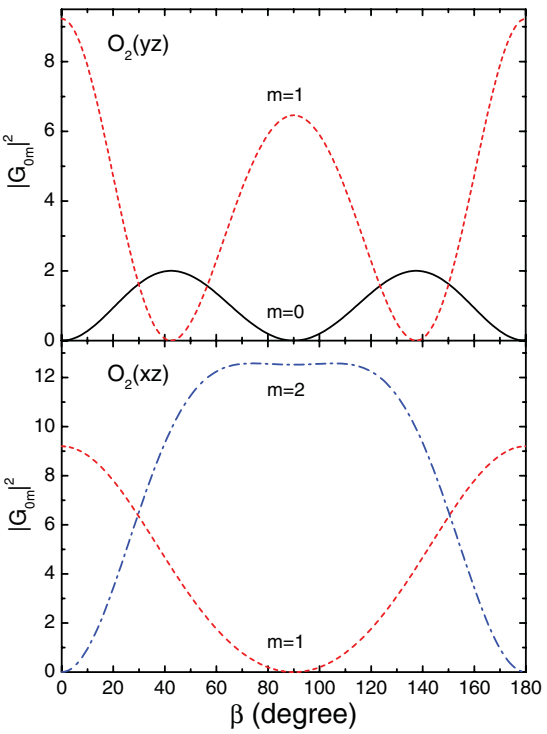

FIG. 5. (Color online) The dependence of the structure factors on the angle β between the internuclear axis and the direction of the electric field [see Eqs. (4) and (5)] for the two degenerate HOMOs in O_2 of π_g symmetry. In the top [bottom] panel $O_2(yz)$ [$O_2(xz)$] denotes that the nodal plane of the π orbital is in the yz [xz] plane. Solid (black) curve, $m = 0$; dashed (red) curve, $m = 1$; dot-dashed (blue) curve, $m = 2$. The nuclei are fixed at the experimental equilibrium distance.

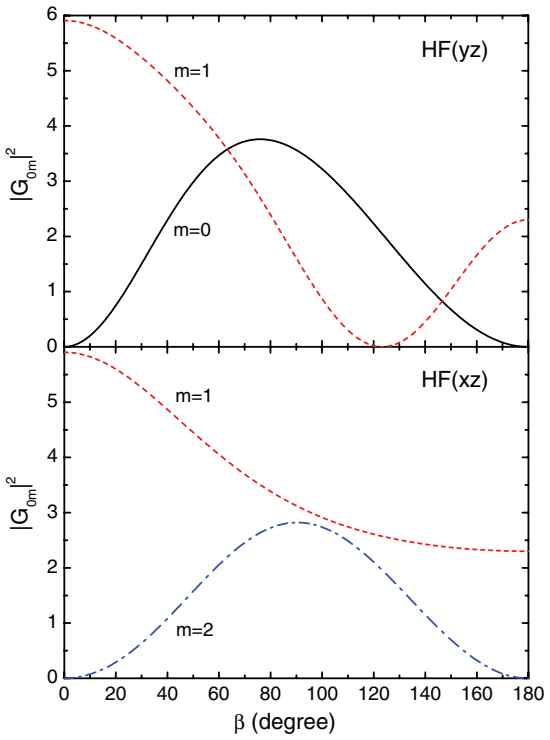

FIG. 6. (Color online) The dependence of the structure factors on the angle β between the internuclear axis and the direction of the electric field [see Eqs. (4) and (5)] for the two degenerate HOMOs in HF of π symmetry. In the top [bottom] panel HF (yz) [HF (xz)] denotes that the nodal plane of the π orbital is in the yz $[xz]$ plane. The H [F] atom is on the negative [positive] z axis in the molecular fixed frame. Solid (black) curve, $m = 0$; dashed (red) curve, $m = 1$; dot-dashed (blue) curve, $m = 2$. The nuclei are fixed at the experimental equilibrium distance.

HOMO of π_g symmetry (see also Fig. 10). In a simple physical picture the shape reflects that most ionization occurs when the orientations with an antinodal surface coincide with the direction of the external field.

Next, in Fig. 6 we show the results for the HOMO of HF with π symmetry and a small permanent dipole moment in the center of mass (see Table III). In the molecular frame (or at $\beta = 0^\circ$) F (H) is on the positive (negative) z axis. It is seen from the figure that $|G_{00}(\beta)|^2$ has a peak at $\beta \simeq 76^\circ$, which is smaller than the angle $\beta \simeq 90^\circ$ predicted by MO-ADK [20] and TDSE calculations within the single-active-electron approximation performed for short pulse with 800 nm and a peak intensity of 2×10^{14} W/cm^2 [20]. The results using the accurate wave functions in the present study led us to conclude that the TDSE study [20] was performed outside the range of applicability of the weak-field asymptotic theory.

The behavior of the rate close to an orientation β_0 where the contribution from the (0,0) channel vanishes requires special consideration. Examples of such β_0's are seen in Fig. 5 at $\beta = 0^\circ, 90^\circ$, and 180° and in Fig. 6 at $\beta = 0^\circ$ and 180°. As discussed in Sec. II, and explicitly contained in Eq. (17), near such an orientation β_0 it is consistent to add the two terms corresponding to the channels (0,0) and (0,1). We illustrate the effect of adding these two terms for the even (yz) HOMO of O_2 in Fig. 7. In the figure, we focus on the ranges of β around

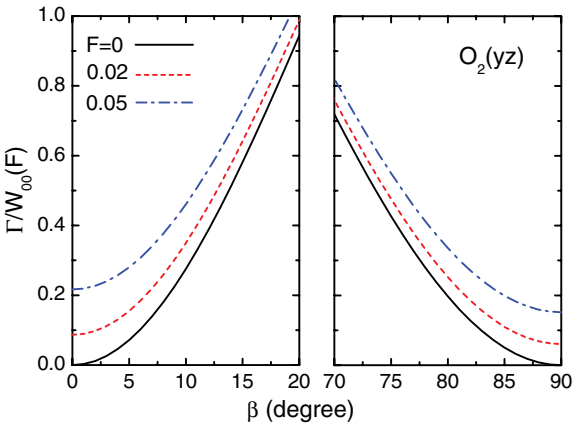

FIG. 7. (Color online) The dependence of the ratio of the rate Γ and the function $W_{00}(F)$ [see Eq. (17)] on the angle β between the internuclear axis and the direction of the electric field for the $O_2(yz)$ HOMO of π_g symmetry near $\beta = 0^\circ$ and $\beta = 90^\circ$, where the contribution to the rate from the (0,0) channel vanishes (see Fig. 5). The different curves show the results for the field strengths indicated. The nuclei are fixed at the experimental equilibrium distance.

0° and 90°. We see that the rate is slightly higher for $\beta = 0^\circ$ than for $\beta = 90^\circ$, which was also found in other theoretical works [12,16,20,21,30,78]. In our theory, the reason for this asymmetry is traced back to the behavior of the structure factor G_{01} (Fig. 5), which attains a higher value for $\beta = 0^\circ$ (and $\beta = 180^\circ$) than for $\beta = 90^\circ$.

We now return to a technical issue and outline briefly the procedure for the extraction of the structure factors $G_{n_\xi m}(\beta)$ from the wave function $\psi_0(\mathbf{r})$ used in the present calculations. The program X2DHF [64,65] accounts very accurately for the asymptotic part of the HOMO for diatomic molecules. Consequently, the integral in Eq. (7) can be reliably calculated for a wide range of η. We do this by using the Laguerre and Chebyshev quadratures for the integrals in ξ and φ, respectively. In this way, the right-hand side of Eq. (7) as a function of η is obtained. As a typical example, we consider the dominant channel (0,0) for the HOMO of $O_2(yz)$. The right-hand side of Eq. (7) as a function of η is shown for several orientations of this molecule by solid curves in Fig. 8. One can see that for each orientation β this function monotonically approaches a constant value as η grows, as it should. To extract this asymptotic constant, we fit the results in the interval $\eta \gtrsim 10$ by an expansion in powers of $1/\eta$. Usually, the coefficients of the first three to four terms can be reliably obtained, which amounts to three to four significant digits in the value of $g_{n_\xi m}(\beta)$. This procedure for calculating the asymptotic coefficients (7) and hence structure factors $G_{n_\xi m}(\beta)$ from the X2DHF wave function is stable for all diatomic molecules considered.

C. Polyatomic molecules: Hartree-Fock wave function using a Gaussian basis

In the case of the diatomic molecules studied above, we used HOMO wave functions from X2DHF with the correct asymptotic behavior [64,65]. Unfortunately, the program X2DHF can only be efficiently implemented for diatomic molecules, since it is based on prolate spheroidal coordinates. For polyatomic

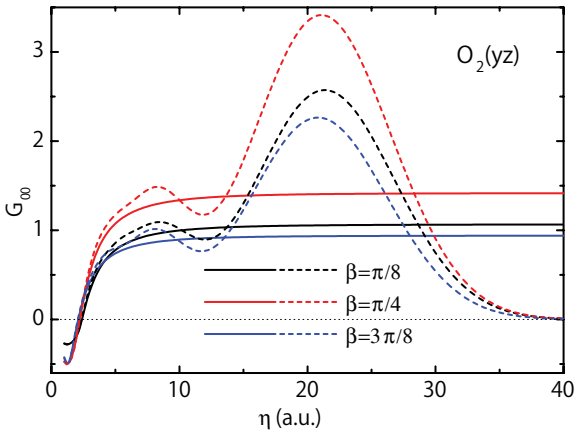

FIG. 8. (Color online) The value of the structure factor $G_{00}(\beta)$ [see Eq. (5)] as a function of η for the $O_2(yz)$ HOMO of π_g symmetry and for three different orientations β of the internuclear axis with respect to the direction of the electric field. Solid curves, using the HOMO wave function obtained by X2DHF [64,65]; dashed curves, using the HOMO wave function obtained by GAMESS [66] with the aug-cc-TZV basis set.

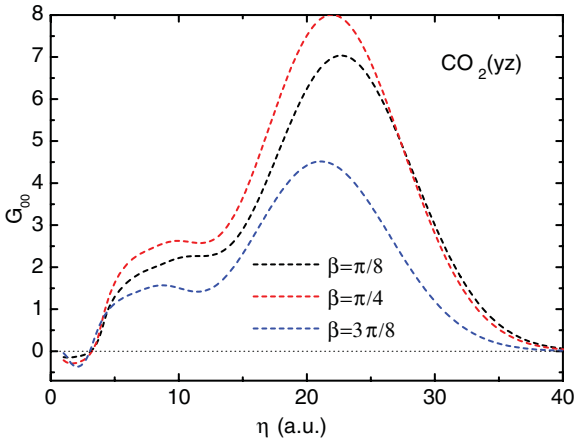

FIG. 9. (Color online) The value of the structure factor $G_{00}(\beta)$ [see Eq. (5)] as a function of η for the $CO_2(yz)$ HOMO of π_g symmetry and for three different orientations β of the internuclear axis with respect to the direction of the electric field. Dashed curves, using the HOMO wave function obtained by GAMESS [66] with the aug-cc-TZV basis set.

molecules the correct asymptotic form can be obtained by a solution of the one-electron Schrödinger equation with a single-active-electron model potential [20–22,25,29]. Here we investigate the prospects for obtaining a good estimate for $G_{00}(\beta)$ directly from conventional quantum chemistry methods expanding the wave function in Gaussians placed at the atomic centers.

To gauge the accuracy of this approach, we return to the results shown in Fig. 8. In the figure, the dashed curves show for different β the structure factor $G_{00}(\beta)$ as a function of η defined by the right-hand side of Eq. (7) obtained using a Hartree-Fock wave function from the quantum chemistry program GAMESS with the aug-cc-TZV basis set [66]. Contrary to the situation when using the X2DHF wave function, the value of $G_{00}(\beta)$ no longer stabilizes for large η, but has a wavy structure and decreases for large η. This lack of convergence is due to the difficulty of representing the asymptotic part of the wave function, which goes like an exponential function, by a sum of Gaussians as used in GAMESS. We have performed similar calculations for all molecules investigated in this work and obtained qualitatively the same results in all cases. In the representative example of Fig. 8 the dashed curves indicate an onset of a plateau for η around 6–7. Using the values for $G_{00}(\beta)$ around the plateau, we estimate that the asymptotic values of $G_{00}(\beta)$ can be extracted within an accuracy of about 20%. With this limit on the accuracy of the structure factors obtained using a Hartree-Fock wave function expressed in a Gaussian basis, we are then ready to move to the consideration of a polyatomic molecule. As a case study we choose CO_2 and use a GAMESS wave function obtained with the aug-cc-TZV basis set. This molecule has attracted considerable attention after the appearance of the experiments [3,4]. In the experiments the ionization yield was found to peak at $\beta \simeq 45°$: in Ref. [3] sharply; in Ref. [4] less sharply. The MO-ADK predicted $\beta \simeq 25°$ [3], or $\beta \simeq 33°$ [18,20–22] depending on the procedure used for the extraction of the entering C_{lm} coefficients. A TDSE result within the single-active-electron approximation predicted $\beta \simeq 45°$ [25], a multiple orbital TDSE calculation at the experimental peak intensity $\beta \simeq 40°$ [30], a multielectron TDSE approach $\beta \simeq 35°$ [26], a mixed position and momentum space approach to tunneling

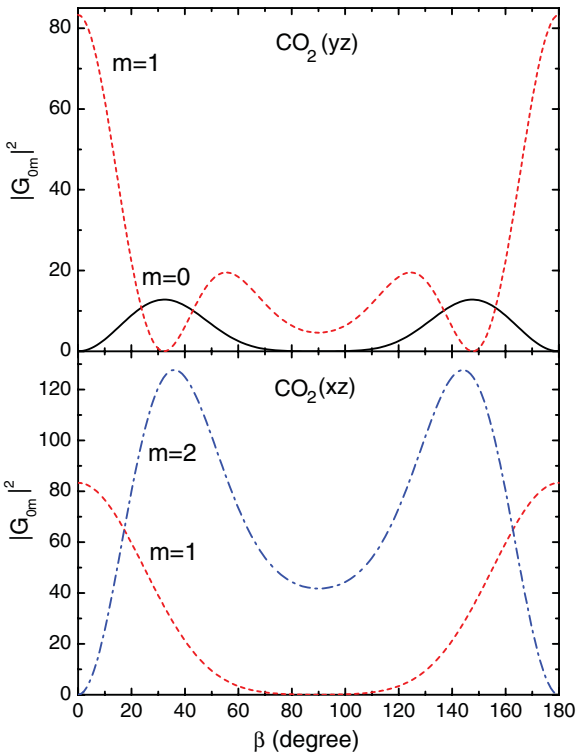

FIG. 10. (Color online) The dependence of the structure factors on the angle β between the internuclear axis and the electric field [see Eqs. (4) and (5)] for the two degenerate HOMOs in CO_2 of π_g symmetry. In the top [bottom] panel $CO_2(yz)$ [$CO_2(xz)$] denotes that the nodal plane of the π orbital is in yz [xz] plane. Solid (black) curve, $m = 0$; dashed (red) curve, $m = 1$; dot-dashed (blue) curve, $m = 2$. The nuclei are fixed at the experimental equilibrium distance.

$\beta \simeq 45^\circ$ [79], and a time-dependent density-functional theory calculation $\beta \simeq 40^\circ$ [28]. Very recent experimental results indicate that contributions from lower-lying orbitals may be involved [80].

As is clear from all these works, the situation is not clarified. Thus it is worth presenting a set of reference data, where the uncertainty can be estimated as explained above. We extracted the asymptotic values of $G_{00}(\beta)$ using the curves as shown in Fig. 9 and plot the results of $|G_{00}(\beta)|^2$ in Fig. 10. Note that the resulting values are subject to an error of about 20% in the extraction of $G_{00}(\beta)$. We see from Fig. 10 that the weak-field asymptotic theory predicts a maximum in the rate at $\beta \simeq 32^\circ$.

IV. CONCLUSIONS AND OUTLOOK

In this work we have demonstrated the application of the weak-field asymptotic theory of tunneling ionization [61] by considering seven linear molecules of current interest. To implement the theory, the initial bound-state orbital from which tunneling occurs is required. In contrast to the situation in much of quantum chemistry, an accurate description of the asymptotic part of the wave function at large η is crucial. For one-electron molecular ions, a virtually exact wave function can be obtained. This case is illustrated by calculations for H_2^+. The benchmark results for this molecule in the weak-field limit are presented. For many-electron molecules, one has to resort to some kind of single-active-electron approximation. For diatomic molecules, it is possible to obtain an accurate wave function in the asymptotic region [64,65]. Apart from an error incurred by the Hartree-Fock approximation, our results for H_2, N_2, O_2, CO, and HF also should be considered as benchmark results in the weak-field limit. In the general case of polyatomic molecules, one needs to rely on standard approaches in quantum chemistry using an expansion of the active orbital in terms of Gaussian basis functions [66]. As illustrated by the examples here, it is tedious with such a basis to obtain an accurate asymptotic form of the wave function beyond, say, $\eta \sim 7$–10. Nevertheless, the experience gained by the detailed comparison with accurate calculations for diatomics allowed us to extract the structure factor for a triatomic molecule CO_2 with an error of $\sim$20%. If this level of accuracy is acceptable, our results show that standard quantum chemistry calculations for the wave function are sufficient. This opens a possibility to apply the theory to bigger molecules of current experimental interest like benzonitrile and naphthalene [11,23], as was demonstrated recently by a study of C_2H_4 [48]. However, if higher accuracy is needed, new reliable methods to construct the wave function in the asymptotic region should be sought. One approach that has already been explored is to construct a single-active-electron model potential from the density-functional theory and calculate the wave function in this potential [20–22,25]. Alternatively, one could start with the wave function from a quantum chemistry code in the region where this function is still accurate and continue it to larger distances by the R-matrix method using the known analytic form of the multipole expansion of the long-range part of the electron-molecule interaction. The exploration of these possibilities for the present theory is left for future studies.

An important issue is an experimental verification of the weak-field asymptotic theory [61] and, on the other hand, its use for the analysis and prediction of the experimental results. First of all, one should clearly realize the range of experimental situations where the theory applies. It is limited by the following: The electric field is assumed to be (i) weak (in the static sense) and (ii) independent of time. Since experimental results on tunneling ionization can be obtained only with time-dependent laser fields, the latter assumption means that the laser frequency ω should be sufficiently low. Tunneling ionization in a time-dependent field $F(t)$ can be treated as that in a static field F equal to the momentary value of $F(t)$ under the condition of applicability of the adiabatic theory [41,81] which for weak fields is $\omega \ll F^2/\varkappa^4$; we note that this is a more stringent condition than the one $\omega \ll F/\varkappa$ defining the tunneling regime of the Keldysh theory [82]. The former assumption means that the laser intensity should be sufficiently low as well, $F \ll \varkappa^3$, but not too low to satisfy the previous condition. An additional condition dictated by the difference between static and oscillating laser fields is that rescattering of ionized electrons should not affect tunneling. Under these conditions, the theory [61] predicts the factorization of the ionization rate (4) into the absolute value squared of the orientation-dependent structure factor $G_{n_\xi m}(\beta,\gamma)$ of Eq. (5) and the field-dependent factor $W_{n_\xi m}(F)$ of Eq. (6). This property suggests an experimental procedure for determining whether a given laser pulse belongs to the range of applicability of the present theory. If the experimental orientation-resolved signal is constant when divided by $W_{n_\xi m}(F)$ of the dominant channel for all laser parameters kept fixed except the intensity, then the present theory applies. If not, then the laser parameters do not satisfy the specified conditions. This should enable one to select suitable experimental conditions and reliably retrieve the target information contained in the structure factor.

ACKNOWLEDGMENTS

This work was supported by the Danish Research Council (Grant No. 10-085430) and by a Grant-in-Aid for scientific research (C) from the Japan Society for the Promotion of Science (JSPS). L.B.M. was also supported by an ERC-StG (Project No. 277767 - TDMET). O.I.T. thanks the Russian Foundation for Basic Research for the support through Grant No. 11-02-00390-a.

[1] I. V. Litvinyuk, K. F. Lee, P. W. Dooley, D. M. Rayner, D. M. Villeneuve, and P. B. Corkum, Phys. Rev. Lett. **90**, 233003 (2003).

[2] A. S. Alnaser, S. Voss, X. M. Tong, C. M. Maharjan, P. Ranitovic, B. Ulrich, T. Osipov, B. Shan, Z. Chang, and C. L. Cocke, Phys. Rev. Lett. **93**, 113003 (2004).

[3] D. Pavičić, K. F. Lee, D. M. Rayner, P. B. Corkum, and D. M. Villeneuve, Phys. Rev. Lett. **98**, 243001 (2007).

[4] I. Thomann, R. Lock, V. Sharma, E. Gagnon, S. T. Pratt, H. C. Kapteyn, M. M. Murnane, and W. Li, J. Phys. Chem. A **112**, 9382 (2008).

[5] H. Akagi, T. Otobe, A. Staudte, A. Shiner, F. Turner, R. Doerner, D. M. Villeneuve, and P. B. Corkum, Science **325**, 1364 (2009).

[6] L. Holmegaard, J. L. Hansen, L. Kalhøj, S. L. Kragh, H. Stapelfeldt, F. Filsinger, J. Küpper, G. Meijer, D. Dimitrovski, M. Abu-samha, and L. B. Madsen, Nat. Phys. **6**, 428 (2010).

[7] D. Dimitrovski, M. Abu-samha, L. B. Madsen, F. Filsinger, G. Meijer, J. Küpper, L. Holmegaard, L. Kalhøj, J. H. Nielsen, and H. Stapelfeldt, Phys. Rev. A **83**, 023405 (2011).

[8] J. L. Hansen, L. Holmegaard, L. Kalhøj, S. L. Kragh, H. Stapelfeldt, F. Filsinger, G. Meijer, J. Küpper, D. Dimitrovski, M. Abu-samha, C. P. J. Martiny, and L. B. Madsen, Phys. Rev. A **83**, 023406 (2011).

[9] H. Ohmura, N. Saito, and T. Morishita, Phys. Rev. A **83**, 063407 (2011).

[10] H. Li, D. Ray, S. De, I. Znakovskaya, W. Cao, G. Laurent, Z. Wang, M. F. Kling, A. T. Le, and C. L. Cocke, Phys. Rev. A **84**, 043429 (2011).

[11] J. L. Hansen, L. Holmegaard, J. H. Nielsen, H. Stapelfeldt, D. Dimitrovski, and L. B. Madsen, J. Phys. B **45**, 015101 (2012).

[12] X. M. Tong, Z. X. Zhao, and C. D. Lin, Phys. Rev. A **66**, 033402 (2002).

[13] T. K. Kjeldsen and L. B. Madsen, J. Phys. B **37**, 2033 (2004).

[14] T. K. Kjeldsen and L. B. Madsen, Phys. Rev. A **71**, 023411 (2005).

[15] T. K. Kjeldsen, C. Z. Bisgaard, L. B. Madsen, and H. Stapelfeldt, Phys. Rev. A **71**, 013418 (2005).

[16] C. Lin and X. Tong, J. Photochem. Photobiol. A **182**, 213 (2006).

[17] A. Staudte, S. Patchkovskii, D. Pavičić, H. Akagi, O. Smirnova, D. Zeidler, M. Meckel, D. M. Villeneuve, R. Dörner, M. Y. Ivanov, and P. B. Corkum, Phys. Rev. Lett. **102**, 033004 (2009).

[18] S.-F. Zhao, C. Jin, A.-T. Le, T. F. Jiang, and C. D. Lin, Phys. Rev. A **80**, 051402 (2009).

[19] X. Chu, Phys. Rev. A **82**, 023407 (2010).

[20] M. Abu-samha and L. B. Madsen, Phys. Rev. A **81**, 033416 (2010).

[21] S.-F. Zhao, C. Jin, A.-T. Le, T. F. Jiang, and C. D. Lin, Phys. Rev. A **81**, 033423 (2010).

[22] S.-F. Zhao, C. Jin, A.-T. Le, and C. D. Lin, Phys. Rev. A **82**, 035402 (2010).

[23] J. L. Hansen, H. Stapelfeldt, D. Dimitrovski, M. Abu-samha, C. P. J. Martiny, and L. B. Madsen, Phys. Rev. Lett. **106**, 073001 (2011).

[24] Y.-J. Jin, X.-M. Tong, and N. Toshima, Phys. Rev. A **83**, 063409 (2011).

[25] M. Abu-samha and L. B. Madsen, Phys. Rev. A **80**, 023401 (2009).

[26] M. Spanner and S. Patchkovskii, Phys. Rev. A **80**, 063411 (2009).

[27] M. Magrakvelidze, F. He, S. De, I. Bocharova, D. Ray, U. Thumm, and I. V. Litvinyuk, Phys. Rev. A **79**, 033408 (2009).

[28] S.-K. Son and S.-I. Chu, Phys. Rev. A **80**, 011403 (2009).

[29] M. Abu-samha and L. B. Madsen, Phys. Rev. A **82**, 043413 (2010).

[30] S. Petretti, Y. V. Vanne, A. Saenz, A. Castro, and P. Decleva, Phys. Rev. Lett. **104**, 223001 (2010).

[31] J. Muth-Böhm, A. Becker, and F. H. M. Faisal, Phys. Rev. Lett. **85**, 2280 (2000).

[32] A. Jaron-Becker, A. Becker, and F. H. M. Faisal, Phys. Rev. A **69**, 023410 (2004).

[33] D. Dimitrovski, C. P. J. Martiny, and L. B. Madsen, Phys. Rev. A **82**, 053404 (2010).

[34] H. B. van Linden van den Heuvell and H. G. Muller, in *Multiphoton Processes*, edited by S. J. Smith and P. L. Knight (Cambrigde University Press, Cambridge, 1988).

[35] T. F. Gallagher, Phys. Rev. Lett. **61**, 2304 (1988).

[36] P. B. Corkum, N. H. Burnett, and F. Brunel, Phys. Rev. Lett. **62**, 1259 (1989).

[37] T. Morishita, A.-T. Le, Z. Chen, and C. D. Lin, Phys. Rev. Lett. **100**, 013903 (2008).

[38] T. Morishita, A.-T. Le, Z. Chen, and C. D. Lin, New J. Phys. **10**, 025011 (2008).

[39] M. V. Frolov, N. L. Manakov, and A. F. Starace, Phys. Rev. A **79**, 033406 (2009).

[40] A. Čerkić, E. Hasović, D. B. Milošević, and W. Becker, Phys. Rev. A **79**, 033413 (2009).

[41] O. I. Tolstikhin, T. Morishita, and S. Watanabe, Phys. Rev. A **81**, 033415 (2010).

[42] M. V. Frolov, N. L. Manakov, T. S. Sarantseva, and A. F. Starace, J. Phys. B **42**, 035601 (2009).

[43] M. V. Frolov, N. L. Manakov, T. S. Sarantseva, and A. F. Starace, Phys. Rev. A **83**, 043416 (2011).

[44] Y. Okajima, O. I. Tolstikhin, and T. Morishita (unpublished).

[45] M. Okunishi, H. Niikura, R. R. Lucchese, T. Morishita, and K. Ueda, Phys. Rev. Lett. **106**, 063001 (2011).

[46] D. Ray, Z. Chen, S. De, W. Cao, I. V. Litvinyuk, A.-T. Le, and C. D. Lin, M. F. Kling, and C. L. Cocke, Phys. Rev. A **83**, 013410 (2011).

[47] C. I. Blaga, J. Xu, A. D. DiChiara, E. Sistrunk, K. Zhang, P. Agostini, T. A. Miller, L. F. DiMauro, C. D. Lin, Nature (London) **483**, 194 (2012).

[48] C. Wang, M. Okunishi, R. R. Lucchese, T. Morishita, O. I. Tolstikhin, L. B. Madsen, K. Shimada, D. Ding, and K. Ueda (unpublished).

[49] S. Minemoto, T. Umegaki, Y. Oguchi, T. Morishita, A.-T. Le, S. Watanabe, and H. Sakai, Phys. Rev. A **78**, 061402 (2008).

[50] C. Jin, A.-T. Le, and C. D. Lin, Phys. Rev. A **83**, 053409 (2011).

[51] P. M. Kraus and H. J. Wörner, Chem. Phys. (2012).

[52] J. R. Oppenheimer, Phys. Rev. **31**, 66 (1928).

[53] P. A. Batishchev, O. I. Tolstikhin, and T. Morishita, Phys. Rev. A **82**, 023416 (2010).

[54] L. D. Landau and E. M. Lifschitz, *Quantum Mechanics (Non-relativistic Theory)* (Pergamon, Oxford, 1977).

[55] Yu. N. Demkov and G. F. Drukarev, Zh. Eksp. Teor. Fiz. **47**, 918 (1964) [Sov. Phys. JETP **20**, 614 (1965)].

[56] B. M. Smirnov and M. I. Chibisov, Zh. Eksp. Teor. Fiz. **49**, 841 (1965) [Sov. Phys. JETP **22**, 585 (1966)].

[57] S. Yu. Slavyanov, Probl. Mat. Fiz. No. 4, 125 (1970) [English translation: *Topics in Mathematical Physics* (Consultants Bureau, New York, London, 1971), Vol. 4].

[58] T. Yamabe, A. Tachibana, and H. J. Silverstone, Phys. Rev. A **16**, 877 (1977).

[59] R. J. Damburg and V. V. Kolosov, J. Phys. B **11**, 1921 (1978).

[60] M. V. Ammosov, N. B. Delone, and V. P. Krainov, Zh. Eksp. Teor. Fiz. **91**, 2008 (1986) [Sov. Phys. JETP **64**, 1191 (1986)].

[61] O. I. Tolstikhin, T. Morishita, and L. B. Madsen, Phys. Rev. A **84**, 053423 (2011).

[62] O. I. Tolstikhin and C. Namba, *CTBC-A Program to Solve the Collinear Three-Body Coulomb Problem: Bound States*

and Scattering Below the Three-Body Disintegration Threshold (National Institute for Fusion Science, Toki, Japan, 2003).
[63] I. V. Komarov, L. I. Ponomarev, and S. Y. Slavyanov, *Spheroidal and Coulomb Spheroidal Functions* (Nauka, Moscow, 1976).
[64] J. Kobus, L. Laaksonen, and D. Sundholm, Comp. Phys. Commun. **98**, 346 (1996).
[65] [http://www.leiflaaksonen.eu/num2d.html].
[66] M. W. Schmidt, K. K. Baldridge, J. A. Boatz, S. T. Elbert, M. S. Gordon, J. H. Jensen, S. Koseki, N. Matsunaga, K. A. Nguyen, S. Su *et al*., J. Comput. Chem. **14**, 1347 (1993).
[67] A. R. Edmonds, *Angular Momentum in Quantum Mechanics* (Princeton University Press, Princeton, 1957).
[68] M. Abramowitz and I. A. Stegun (Editors), *Handbook of Mathematical Functions* (Dover, New York, 1972).
[69] E. U. Condon and G. H. Shortley, *Theory of Atomic Spectra* (Cambridge University Press, Princeton, 1935).
[70] G. L. Kamta and A. D. Bandrauk, Phys. Rev. A **71**, 053407 (2005).
[71] D. A. Telnov and S. I. Chu, Phys. Rev. A **76**, 043412 (2007).
[72] Nist Standard Reference Database 101. Computational Chemistry Comparison and Benchmark Database (2011).
[73] J. W. Robinson, ed., *Handbook of Spectroscopy* (CRC, Cleveland, OH, 1974).
[74] D. A. Telnov and S. I. Chu, Phys. Rev. A **80**, 043412 (2009).
[75] E. Hasović, M. Busuladžić, W. Becker, and D. B. Milošević, Phys. Rev. A **84**, 063418 (2011).
[76] A. N. Pfeiffer, C. Cirelli, M. Smolarski, D. Dimitrovski, M. Abusamha, L. B. Madsen, and U. Keller, Nat. Phys. **8**, 76 (2012).
[77] N. I. Shvetsov-Shilovski, D. Dimitrovski, and L. B. Madsen, Phys. Rev. A **85**, 023428 (2012).
[78] D. A. Telnov and S.-I. Chu, Phys. Rev. A **79**, 041401 (2009).
[79] R. Murray, M. Spanner, S. Patchkovskii, and M. Y. Ivanov, Phys. Rev. Lett. **106**, 173001 (2011).
[80] C. Wu, H. Zhang, H. Yang, Q. Gong, D. Song, and H. Su, Phys. Rev. A **83**, 033410 (2011).
[81] O. I. Tolstikhin and T. Morishita (unpublished).
[82] L. V. Keldysh, Zh. Eksp. Teor. Fiz. **47**, 1945 (1964) [Sov. Phys. JETP **20**, 1307 (1965)].